Supporting Information for:

Selective Electrochemical Capture and Release of Uranyl from Aqueous Alkali, Lanthanide, and Actinide Mixtures using Redox-Switchable Carboranes

Megan Keener,[a] Maxwell Mattejat,[a] Shao-Liang Zheng,[b] Guang Wu,[a] Trevor Hayton,[a] and Gabriel Ménard*[a]

[a]Department of Chemistry and Biochemistry, University of California, Santa Barbara, California 93106, USA.
[b]Department of Chemistry and Chemical Biology, Harvard University, Cambridge, Massachusetts 02138, USA.

Table of Contents

S1. Materials and Physical Measurements

General Considerations

All manipulations were performed under an atmosphere of dry, oxygen-free N_2 or Ar by means of standard Schlenk or glovebox techniques (MBraun, equipped with a -38 °C freezer, or VAC gloveboxes). Hexanes, pentane, dichloromethane (DCM), and benzene were dried on an MBraun solvent purification system. Acetonitrile ($–H_3$ and $–D_3$) was dried over CaH_2 for several days prior to distillation. THF was dried over sodium benzophenone and distilled. 1,2-Dichloroethane (DCE) was initially distilled followed by drying over CaH_2 for several days prior to a second distillation and subsequent storage on activated 4 Å molecular sieves. $[Bu_4N][Cl]$ was purchased from Fisher Scientific. $[Th(NO_3)_4•H_2O]$ was purchased from Stream Chemicals. *Ortho*-carborane was purchased from Boron Specialties and sublimed before use. Ph_2PCl was purchased from Aldrich and vacuum distilled prior to use. $CsNO_3$ and decamethylcobaltocene ($CoCp_2^*$) were purchased from Aldrich. $CoCp_2^*$ was purified by filtration through Celite using pentane, followed by recrystallization from pentane at -38 °C over several days. $[Bu_4N][PF_6]$ was purchased from Oakwood Chemicals and purified by twice recrystallizing from hot ethanol. The recrystallized product was then washed with cold water, cold ethanol, and pentane prior to drying at 100 °C under vacuum for 24 h. Sodium acetate (NaOAc) buffers (0.1 and 0.5 M) were prepared from a stock solution purchased from Aldrich (pH 4.9) and adjusted to pH 5.4 using NaOH. The pH value was confirmed using a pH meter. Ketjenblack® EC-600JD (KB) was purchased from a private supplier. $UO_2(NO_3)_2(THF)_2$,[1] $Nd(NO_3)_3(THF)_3$,[2] KC_8,[3] $[Ph_3PNPPh_3][PF_6]$,[4] and compounds **^{PO}Cb**, **$[CoCp_2^*]_2[^{PO}Cb]$**, and **$[Bu_4N]_2[^{PO}Cb]$** were prepared using literature procedures.[5] The synthesis of $Sm(NO_3)_3(THF)_3$ was adapted from the synthesis of $Nd(NO_3)_3(THF)_3$.[2]

Physical Measurements

NMR spectra were obtained on a Varian Unity Inova 500 MHz or Agilent Technologies 400 MHz spectrometer, and referenced to residual solvent resonances of acetonitrile (MeCN-d_3) or externally (^{11}B: 85% $(Et_2O)BF_3$, ^{31}P: 85% H_3PO_4,). Unlocked spectra were collected with the ^2H lock turned off. Gradient shimming including Z1 to Z5 was done with the strong ^1H signal in the samples using a shim map generated with the same or similar sample with equal sample volume. Chemical shifts (δ) are recorded in ppm. All ^{11}B NMR spectra were processed using MestReNova software in order to reduce background signal with a linewidth of approximately 3000 Hz from the Pyrex NMR tubes. The NMR time-domain data were first left-shifted to discard the first ~0.1 ms. To correct the linear phase change, linear prediction (LP) is used to fill the initial discarded data before Fourier transform or an appropriate linear phase correction is applied to the frequency domain data after Fourier transform. T_1 relaxation values for ^{31}P nuclei were determined using the inversion-recovery method. The delay times after the 180-degree inversion pulse were varied up to the maximum of 5 times of the expected T_1 values. T_1 values for complexes **^{PO}Cb**, **$[CoCp^*_2]_2[^{PO}Cb]$**, **$[Bu_4N]_2[^{PO}Cb]$**, **$[CoCp^*_2]_2[UO_2Cl_2{}^{PO}Cb]$**, **$[CoCp^*_2]_2[UO_2(^{PO}Cb)_2]$**, and $[Ph_3PNPPh_3][PF_6]$ were determined in our previous report.[5]

Elemental analyses (C, N, H) were recorded at the University of California, Berkeley using a Perkin Elmer 2400 Series II combustion analyser.

Galvanostatic Bulk Electrolysis cycling experiments were carried out using a Metrohm Autolab PGSTAT128N potentiostat/galvanostat and carried out inside an Ar glovebox. The full experimental setup for both the mono- and biphasic cycling experiments are described below.

X-ray crystallography data for complexes **$[[CoCp^*_2][Cs(^{PO}Cb)]]_2$**, **$[CoCp^*_2]_3[Nd(^{PO}Cb)_3]$**, and **$[CoCp^*_2]_2[Th(^{PO}Cb)_3]$** were collected at the University of California, Santa Barbara on a Bruker KAPPA APEX II diffractometer equipped with an APEX II CCD detector using a TRIUMPH monochromator with a Mo Kα X-ray source (α = 0.71073 Å). The crystals were mounted on a cryoloop under Paratone-N oil, and all data were collected at 100(2) K using an Oxford nitrogen gas cryostream system. A hemisphere of data was collected using ω scans with 0.5° frame widths. Data collection and cell parameter determination were conducted using the SMART program. Integration of the data frames and final cell parameter refinement were performed using SAINT software. Absorption correction of the data was carried out using SADABS. Structure determination was done using direct or Patterson methods and difference Fourier techniques. All hydrogen atom positions were idealized and rode on the atom of attachment. Structure solution, refinement, graphics, and creation of publication materials were performed using SHELXTL or

OLEX2. XRD studies for complexes **$[CoCp^*_2]_3[Sm(^{PO}Cb)_3]$** and **$[Bu_4N][^{PO}CbH]$** were carried out at Harvard University and the data was collected at 100 K. The intensities of the reflections were collected by means of a Bruker D8 Venture diffractometer (MoKα radiation, λ=0.71073 Å), and equipped with an Oxford Cryosystems nitrogen flow apparatus. The collection method involved 0.5° scans in ω at 0, and 29° in 2θ with a Photon100 detector distance at 10 cm. Data integration down to 0.84 Å resolution was carried out using SAINT V8.37A with reflection spot size optimization. Absorption corrections were made with the program SADABS. The structure was solved by the Intrinsic Phasing methods and refined by least-squares methods again F2 using SHELXT-2014 and SHELXL-2014[6, 7] with OLEX2 interface.[8] Non-hydrogen atoms were refined anisotropically, and hydrogen atoms were allowed to ride on the respective atoms.

Inductively Coupled Plasma-Optical Emission Spectroscopy (ICP-OES) was performed on a Agilent 5800 and used to determine the concentrations of Th, Nd, Sm, Cs, and U in aqueous solutions. Nitric acid (Thermo Scientific, ICP-OES grade for trace metal analysis, ACS testing specifications, LOT 211316) and deionized water (Milli-Q, 18.2 MΩ.cm) were used for sample preparation and dilutions. A seven-point calibration curve was made by serial dilution (100- 0.01 ppm) of a custom multi-element certified reference material from High Purity Standards in 2% nitric acid. The emissions lines used were Th (269.242 nm, 274.716 nm, 283.730 nm), Nd (401.224 nm, 406.108 nm, 410.945 nm, 430.357 nm), Sm (356.827 nm, 359.259 nm, 360.949 nm, 446.734 nm), Cs (697.327 nm) and U (263.553 nm, 367.007 nm, 385.957 nm). The calibrations curves for Th, Nd, Sm and U all had $R^2 > 0.9999$. A six-point calibration curve was used for Cs with a $R^2 > 0.998$, due to an interference in the 0.01 ppm standard.

S2. Synthesis of Compounds

Synthesis of $[[CoCp^*_2][Cs(^{PO}Cb)]]_2$: A 20 mL vial equipped with a magnetic stir bar was charged with $CsNO_3$ (4.0 mg, 0.02 mmol) and 1 mL of MeCN. In a separate vial, **$[CoCp^*_2]_2[^{PO}Cb]$** (24.0 mg, 0.02 mmol) was dissolved in 2 mL of MeCN and then added dropwise to the stirring solution of $CsNO_3$, where the solution went from golden to bright yellow. The solution remained homogenous and the reaction was stirred at room temperature for 2 h. The solution was filtered over Celite and the volatiles were removed *in vacuo*, yielding a shiny golden solid. Residual [CoCp$^*_2$][NO$_3$] was removed from this crude yellow solid by repeated selective recrystallizations (2-3 times) by vapor diffusion of Et$_2$O into a concentrated pyridine solution of the crude solid at -38 °C. The supernatant was then transferred and the volatiles removed yielding a yellow solid (10.3 mg, 0.010 mmol, 51 % yield). Single crystals suitable for XRD studies were grown by vapor diffusion of Et$_2$O into a saturated MeCN solution of **[[CoCp$^*_2$][Cs(^{PO}Cb)]]$_2$** at room temperature yielding large golden blocks. **^{1}H NMR** (400 MHz, MeCN-*d$_3$*): δ 7.88 (m, 16H); 7.26 (m, 24H); 1.69 (s, 60H). Note: Carborane B–**H** resonances are too broad to be observed. **^{11}B{^{1}H} NMR** (128 MHz, MeCN-*d$_3$*): δ 21.01; -0.49; -18.91; -21.60. **^{31}P{^{1}H} NMR** (162 MHz, MeCN-*d$_3$*): δ 31.66. *Anal. Calcd*. for $C_{45}H_{60}B_{10}CoO_2P_2SCs$: C, 54.87; H, 6.01. *Found*: C, 54.68; H, 6.04.

Synthesis of [CoCp$^*_2$]$_3$[Nd(^{PO}Cb)$_3$]: A 20 mL vial equipped with a magnetic stir bar was charged with **[CoCp$^*_2$]$_2$[^{PO}Cb]** (36.0 mg, 0.03 mmol) and 2 mL of MeCN. In a separate vial, [Nd(NO$_3$)$_3$(THF)$_3$] (5.4 mg, 0.01 mmol) was dissolved in 2 mL of MeCN and then added dropwise to the stirring solution of **[CoCp$^*_2$]$_2$[^{PO}Cb]**, where the solution went from golden to bright yellow. The solution remained homogenous and the reaction was stirred at room temperature for 2 h. The volatiles were removed *in vacuo*, yielding a yellow powder. The powder was washed with THF (8 mL) and the mixture was transferred onto a bed of Celite on a glass frit. The yellow solid was washed with additional THF (3 x 2 mL). The filter was then dissolved in MeCN into a new vial. The MeCN filtrate was collected and the volatiles removed *in vacuo*, yielding a yellow powder. Residual [CoCp$^*_2$][NO$_3$] was removed from this crude yellow solid by repeated selective recrystallizations (2-3 times) by vapor diffusion of Et$_2$O into a concentrated pyridine solution of the crude solid at -38 °C. The supernatant was then transferred and the volatiles removed yielding a yellow solid (18.2 mg, 0.0066 mmol, 66 % yield). Single crystals suitable for XRD studies were grown by vapor diffusion of Et$_2$O into a saturated MeCN solution of **[CoCp$^*_2$]$_3$[Nd(^{PO}Cb)$_3$]** at room temperature. **^{1}H NMR** (400 MHz, MeCN-*d$_3$*): δ 9.82 (broad m, 14H); 7.64 (m, 15H); 7.34 (m, 8H); 5.42 (s, 8H); 4.13 (s, 15H); 1.68 (s, 90H). Note: Carborane B–**H** resonances are too broad to be observed. **^{11}B{^{1}H}**

NMR (128 MHz, MeCN-d_3): δ 0.17; -17.57. **^{31}P{^{1}H} NMR** (162 MHz, MeCN-d_3): δ 140.6. *Anal. Calcd.* for $C_{130}H_{168}N_6B_{30}O_6P_6Co_2Nd$: C, 58.20; H, 6.31; N, 3.13. *Found*: C, 58.39; H, 6.96; N, 3.13.

Synthesis of [CoCp$^*_2$]$_3$[Sm(^{PO}Cb)$_3$]: A 20 mL vial equipped with a magnetic stir bar was charged with **[CoCp$^*_2$]$_2$[^{PO}Cb]** (24.0 mg, 0.02 mmol) and 2 mL of MeCN. In a separate vial, [Sm(NO_3)$_3$(THF)$_3$] (3.6 mg, 0.0066 mmol) was dissolved in 2 mL of MeCN and then added dropwise to the stirring solution of **[CoCp$^*_2$]$_2$[^{PO}Cb]**, where the solution went from golden to bright yellow. The solution remained homogenous and the reaction was stirred at room temperature for 2 h. The volatiles were removed *in vacuo*, yielding a yellow powder. The powder was washed with THF (8 mL) and the mixture was transferred onto a bed of Celite on a glass frit. The yellow solid was washed with additional THF (3 x 2 mL). The filter was then dissolved in MeCN into a new vial. The MeCN filtrate was collected and the volatiles removed *in vacuo*, yielding a yellow powder. Residual [CoCp$^*_2$][NO_3] was removed from this crude yellow solid by repeated selective recrystallizations (2-3 times) by vapor diffusion of Et_2O into a concentrated pyridine solution of the crude solid at -38 °C. The supernatant was then transferred and the volatiles removed yielding a yellow solid (12.1 mg, 0.0044 mmol, 66 % yield). Single crystals suitable for XRD studies were grown by vapor diffusion of Et_2O into a saturated MeCN solution of **[CoCp$^*_2$]$_3$[Sm(^{PO}Cb)$_3$]** at room temperature. **^{1}H NMR** (400 MHz, MeCN-d_3): δ 8.86 (t, *J* = 9.1 Hz, 12H); 7.24 (bt, *J* = 9.1 Hz, 12H); 7.12 (t, *J* = 7.4 Hz, 6H); 6.25 (t, *J* = 7.4 Hz, 6H); 5.84 (t, *J* = 9.1 Hz, 12H); 5.35 (bt, *J* = 7.4 Hz, 12H); 1.69 (s, 90H). Note: Carborane B–**H** resonances are too broad to be observed. **^{11}B{^{1}H} NMR** (128 MHz, MeCN-d_3): δ 0.04; -17.00; -18.15. **^{31}P{^{1}H} NMR** (162 MHz, MeCN-d_3): δ 27.87. *Anal. Calcd.* for $C_{138}H_{180}B_{30}Co_3O_6P_6Sm$: C, 59.79; H, 6.54. *Found*: C, 59.51; H, 6.12.

Synthesis of [CoCp$^*_2$]$_2$[Th(^{PO}Cb)$_3$]: A 20 mL vial equipped with a magnetic stir bar was charged with **[CoCp$^*_2$]$_2$[^{PO}Cb]** (24.0 mg, 0.02 mmol) and 2 mL of MeCN. In a separate vial, [Th(NO_3)$_4$•H_2O] (3.4 mg, 0.0066 mmol) was dissolved in 1 mL of MeCN and then added dropwise to the stirring solution of **[CoCp$^*_2$]$_2$[^{PO}Cb]**, where the solution went from golden to bright yellow. After stirring for 5 mins, a yellow solid began to precipitate from the reaction mixture. The mixture was stirred at room temperature for an additional 2 h. Stirring was discontinued and the mixture was filtered on Celite and yielding a yellow solid and a yellow filtrate. The solvent was removed from the yellow filtrate yielding a yellow solid. Residual $[CoCp^*_2][NO_3]$ was removed from this crude yellow solid by repeated selective recrystallizations (2-3 times) by vapor diffusion of Et_2O into a concentrated pyridine solution of the crude solid at -38 °C. The supernatant was then transferred and the volatiles removed yielding a yellow solid (7.1 mg, 0.0029 mmol, 44 % yield). Single crystals suitable for XRD studies were grown by vapor diffusion of Et_2O into a saturated MeCN solution of **$[CoCp^*_2]_2[Th(^{PO}Cb)_3]$** at room temperature. **^{1}H NMR** (400 MHz, MeCN-*d_3*): δ 7.95 (m, 12H); 7.84 (m, 12H); 7.09 (m, 18H); 6.87 (t, 6H); 6.15 (m, 12H); 1.69 (s, 60H). Note: Carborane B–**H** resonances are too broad to be observed. **^{11}B{^{1}H} NMR** (128 MHz, MeCN-*d_3*): δ 0.85; -17.57. **^{31}P{^{1}H} NMR** (162 MHz, MeCN-*d_3*): δ 51.32. *Anal. Calcd*. for $C_{115}H_{141}B_{30}Co_2O_6P_6Th$: C, 55.7; H, 5.73. *Found*: C, 54.09; H, 5.72. (Unfortunately, multiple attempts to obtain satisfactory analyses consistently returned a low C value, perhaps due to incomplete combustion).

Synthesis of $[Bu_4N][^{PO}CbH]$: A 1.5 mL NaOAc buffered aqueous solution (0.5 M, pH 5.4) was added slowly dropwise without stirring to a DCE solution (4 mL) containing **$[Bu_4N]_2[^{PO}Cb]$** (20.5 mg, 0.02 mmol). After addition, the mixture was allowed to stir for 2.5 h, after which stirring was discontinued and the organic and aqueous phases were separated using a small separatory funnel. The DCE fraction was collected and the volatiles were removed *in vacuo*, yielding a colorless oil. The product was selectively recrystallized by diffusion of pentane into a saturated THF solution containing a mixture of **$[Bu_4N][^{PO}CbH]$** and **^{PO}Cb** at room temperature. The solution, containing **^{PO}Cb**, was decanted off and the colorless crystalline solid **$[Bu_4N][^{PO}CbH]$** was collected (9.4 mg, 0.012 mmol, 60 % yield). Crystals suitable for XRD studies were obtained by repeated recrystallization through vapor diffusion of pentane into a saturated solution of **$[Bu_4N][^{PO}CbH]$** in THF at room temperature. **^{1}H NMR** (400 MHz, $CDCl_3$): δ 8.05 (m, 4H); 7.56 (m, 4H); 7.35 (m, 8H); 7.24 (m, 4H); 4.27 (broad s, 1H); 3.19 (broad m, 8H); 1.58 (broad m, 8H); 1.38 (broad m, 8H); 0.94 (t, 12H). Note: Carborane B–**H** resonances are too broad to be observed. **^{11}B{^{1}H} NMR**

(128 MHz, $CDCl_3$): δ 16.58; 2.18; -5.29; -14.79; -20.64. **$^{31}P\{^1H\}$ NMR** (162 MHz, $CDCl_3$): δ 27.5, 24.7. *Anal. Calcd*. for $C_{42}H_{66}B_{10}NO_2P_2$: C, 64.10; H, 8.54; N, 1.78. *Found*: C, 63.74; H, 8.27; N, 1.71.

S3. Biphasic Electrochemical Capture and Release of UO_2^{2+}

S3.1. Experimental Conditions

Two-electrode galvanostatic bulk electrolysis (GBE) was performed in an argon glovebox utilizing a two compartment H-cell with a glass frit separator, a stir bar in each compartment, and reticulated vitreous carbon (RVC) foam electrodes for both the working and counter electrodes (**Figure S1**). The RVC foam electrodes consisted of a ~5 cm steel rod inserted into 100 PPI Duocel® RVC foam core (length ~3 cm; diameter ~3 mm), with a tap bore (length ~5 mm; diameter ~2 mm), which was filled with molten gallium to fuse the steel connector to the RVC foam. Each electrode has an end-to-tip resistance of < 10 Ω. The RVC electrodes were rinsed with methanol and dried under reduced pressure overnight prior to use. The Ketjenblack used was dried for 48 h in a 175 °C oven and ground in a glass mortar and pestle under inert atmosphere prior to use.[5]

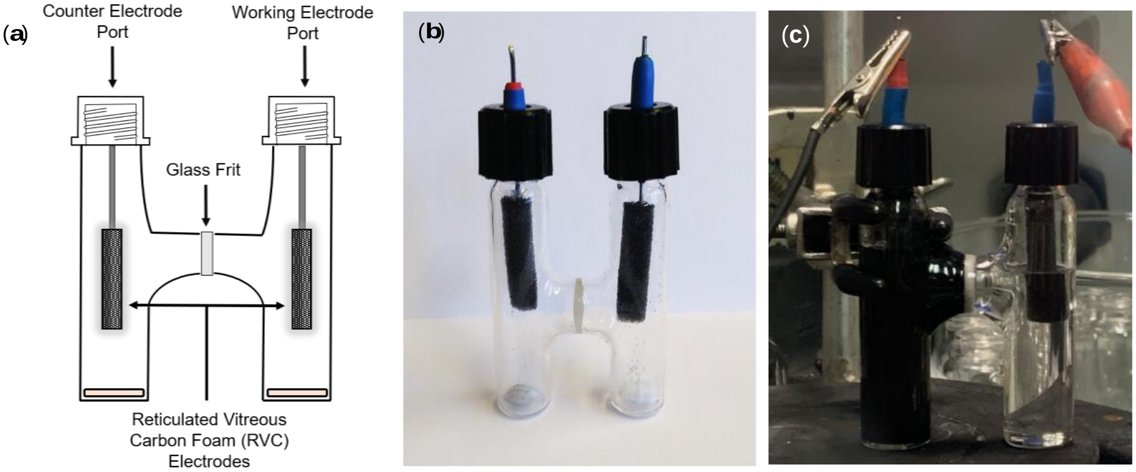

Figure S1. H-Cell Design. (a) Schematic of the two-compartment H-cell used for the biphasic electrochemical separation and recovery of UO_2^{2+}. (b) Picture of the two-compartment H-cell used for the biphasic electrochemical separation and recovery of UO_2^{2+}. (c) Experimental setup of H-cell (before charging) used for the biphasic separation and recovery.

S3.2. Experimental Methods

Reduction (Charging): The counter compartment consisted of 300 mg of Ketjenblack suspended in 8 mL of a 0.1 M solution of $[Bu_4N][PF_6]$ in DCE. The working compartment consisted of $\mathbf{^{PO}Cb}$ (34.3 mg, 0.063 mmol, 1.0 equiv) and $[Ph_3PNPPh_3][PF_6]$ (21.7 mg, 0.032 mmol, 0.5 equiv) dissolved in 6 mL of a 0.1 M solution of $[Bu_4N][PF_6]$ in DCE. An initial $^{31}P\{^1H\}$ NMR spectrum was obtained of the DCE layer (**Figure S2a-S4a**). A charging current of -107.1 μA with a -9.25 C charge cutoff was utilized, resulting in a ca. 76% SOC after 24 h assuming 100% columbic efficiency (**Figure S5**). Upon completion, the working compartment solution was analyzed by $^{31}P\{^1H\}$ NMR spectroscopy to reveal the formation of $\mathbf{[^{PO}Cb]^{2-}}$ with some remaining $\mathbf{^{PO}Cb}$ (**Figure S2b-S4b**). Based on $[Ph_3PNPPh_3][PF_6]$, the amount of $\mathbf{[^{PO}Cb]^{2-}}$ was determined to be 0.0479 mmol (76% yield). The working compartment solution was then removed from the H-cell and placed in a 20 mL vial for subsequent selective UO_2^{2+} capture chemistry.

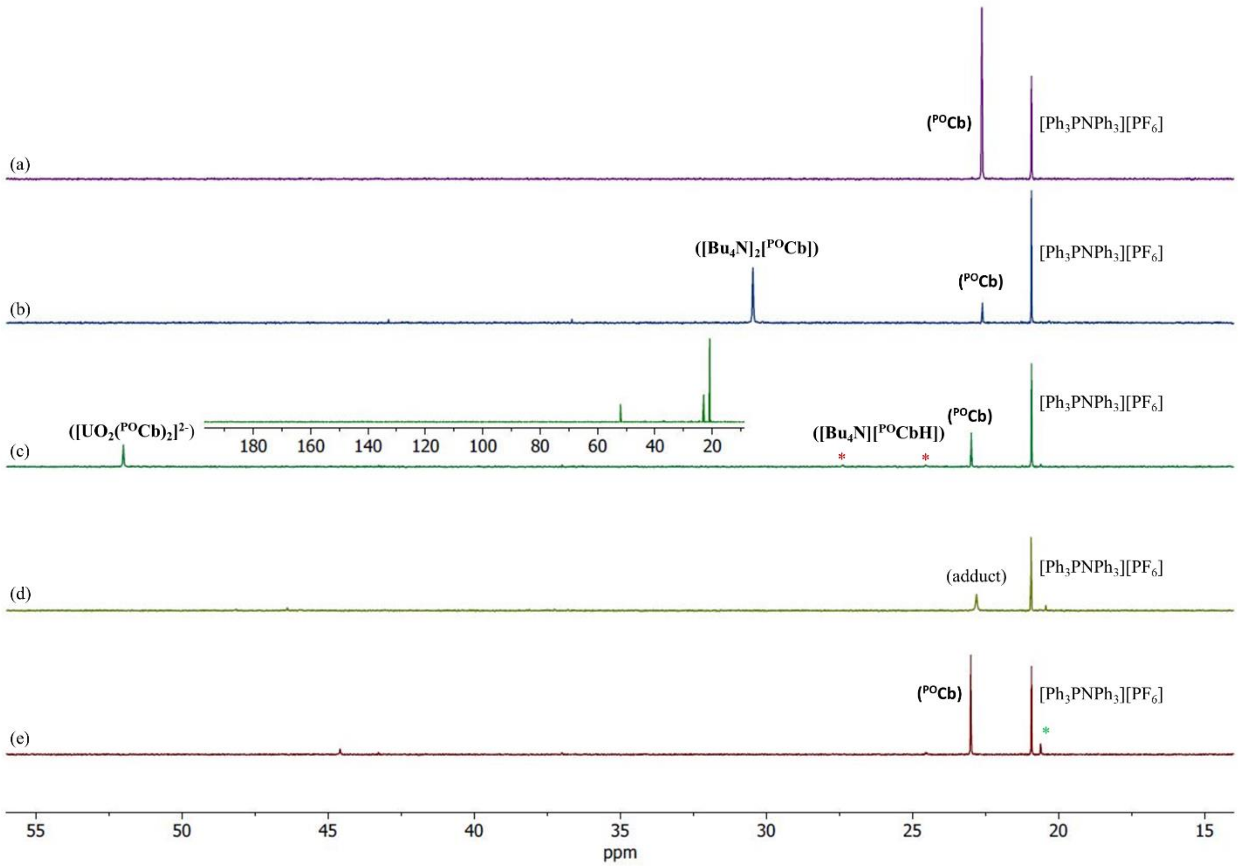

Figure S2. ^{31}P{^{1}H} NMR Spectra for the Electrochemical Capture and Release of UO_2^{2+} from a 1.25 Equiv Mixed Metal Aqueous Solution. (a) Initial unlocked ^{31}P{^{1}H} NMR spectrum of **^{PO}Cb** and $[Ph_3PNPPh_3][PF_6]$ in DCE. (b) ^{31}P{^{1}H} NMR spectrum of the DCE layer following GBE charging generating the reduced **$[^{PO}Cb]^{2-}$** and some residual **^{PO}Cb**. (c) ^{31}P{^{1}H} NMR spectrum of DCE layer following the selective UO_2^{2+} capture from the aqueous layer containing $UO_2(NO_3)_2(THF)_2$, $Th(NO_3)_4$•H_2O, $Nd(NO_3)_3THF_3$, $Sm(NO_3)_3THF_3$, and $CsNO_3$ (pH = 2.6), indicating the formation of **$[UO_2(^{PO}Cb)_2]^{2-}$**, as well as some minor **^{PO}Cb** and **$[Bu_4N][^{PO}CbH]$** (denoted as *). No resonances attributable to the captured metal anions, **$[Cs(^{PO}Cb)]^-$** (31.7 ppm), **$[Nd(^{PO}Cb)_3]^{3-}$** (140.6 ppm), **$[Sm(^{PO}Cb)_3]^{3-}$** (27.9 ppm), or **$[Th(^{PO}Cb)_3]^{2-}$** (51.3 ppm), are observed (inset). (d) ^{31}P{^{1}H} NMR spectrum of the DCE layer following GBE discharging revealing a very broad resonance at 23 ppm which we attribute to an adduct of UO_2^{2+} with **^{PO}Cb**.[5] (e) ^{31}P{^{1}H} NMR spectrum of the DCE layer following UO_2^{2+} release by mixing with Milli-Q water after 15 h and revealing the free carborane **^{PO}Cb** (major), as well as an unknown by-product at 20 ppm, marked by *.

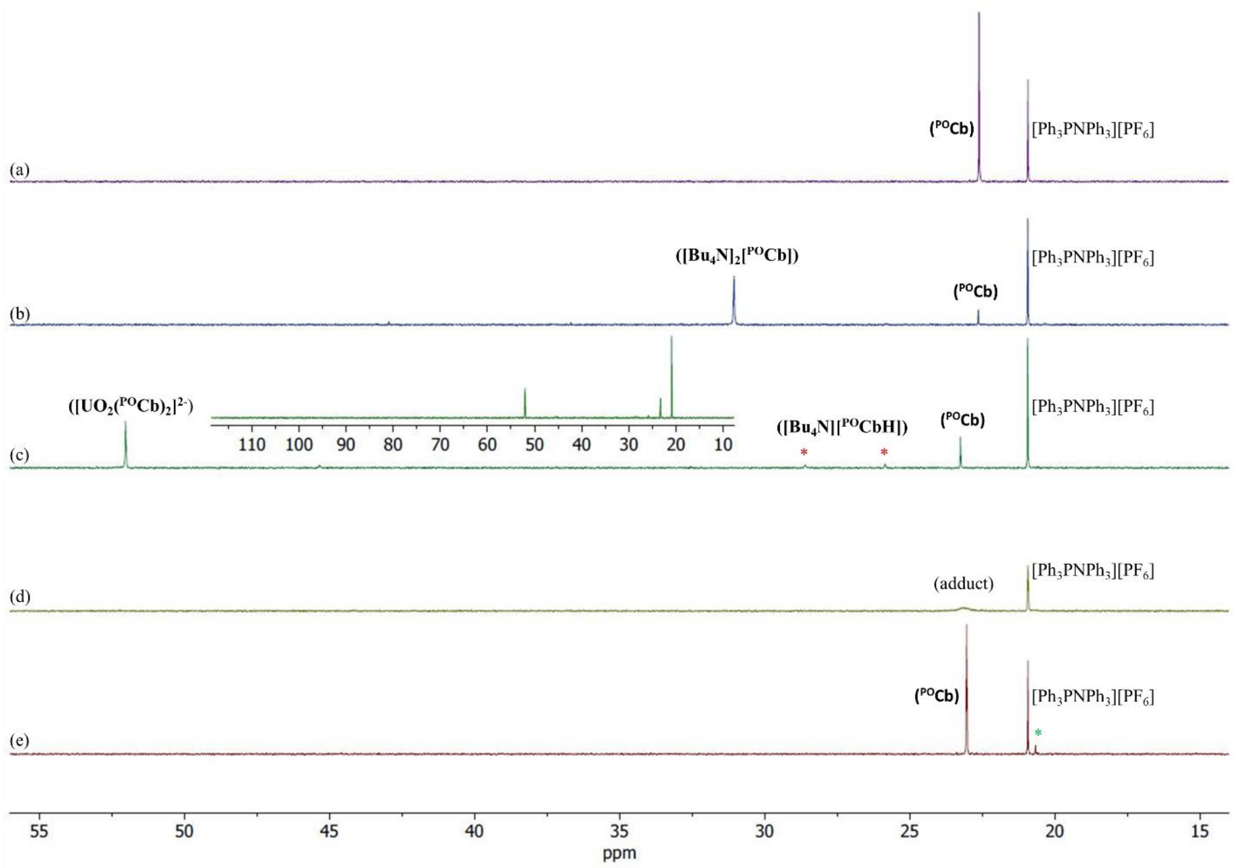

Figure S3. ^{31}P{^{1}H} NMR Spectra for the Electrochemical Capture and Release of UO_2^{2+} from a 1.25 Equiv Mixed Metal Buffered Aqueous Solution. (a) Initial unlocked ^{31}P{^{1}H} NMR spectrum of **^{PO}Cb** and [Ph_3PNPPh_3][PF_6] in DCE. (b) ^{31}P{^{1}H} NMR spectrum of the DCE layer following GBE charging generating the reduced **[^{PO}Cb]$^{2-}$** and some residual **^{PO}Cb**. (c) ^{31}P{^{1}H} NMR spectrum of DCE layer following the selective UO_2^{2+} capture from the aqueous layer containing $UO_2(NO_3)_2(THF)_2$, $Th(NO_3)_4$•H_2O, $Nd(NO_3)_3THF_3$, $Sm(NO_3)_3THF_3$, and $CsNO_3$ in 0.5 M NaOAc buffer (pH = 5.4), indicating the formation of **[UO_2(^{PO}Cb)$_2$]$^{2-}$**, as well as some minor **^{PO}Cb** and **[Bu_4N][^{PO}CbH]** (denoted as *). No resonances attributable to the captured metal anions, **[Cs(^{PO}Cb)]$^-$** (31.7 ppm), **[Nd(^{PO}Cb)$_3$]$^{3-}$** (140.6 ppm), **[Sm(^{PO}Cb)$_3$]$^{3-}$** (27.9 ppm), or **[Th(^{PO}Cb)$_3$]$^{2-}$** (51.3 ppm), are observed (inset). (d) ^{31}P{^{1}H} NMR spectrum of the DCE layer following GBE discharging revealing a very broad resonance at 23 ppm which we attribute to an adduct of UO_2^{2+} with **^{PO}Cb**.[5] (e) $^{31}P\{^1H\}$ NMR spectrum of the DCE layer following UO_2^{2+} release by mixing with fresh NaOAc buffered solution (0.1 M) after 15 h and revealing the free carborane **^{PO}Cb** (major), as well as an unknown by-product at 20 ppm, marked by *.

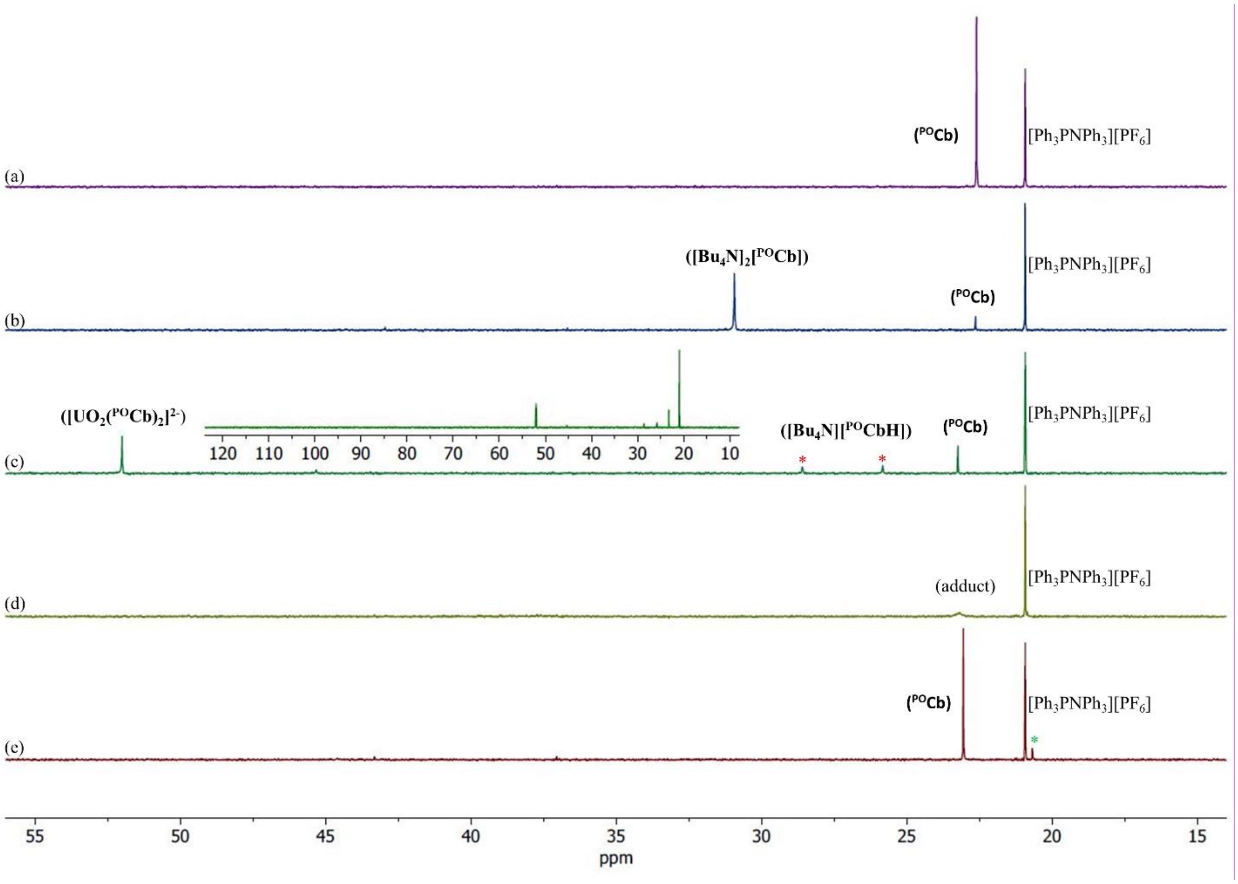

Figure S4. $^{31}P\{^1H\}$ NMR Spectra for the Electrochemical Capture and Release of UO_2^{2+} from a 0.6 Equiv Mixed Metal Buffered Aqueous Solution. (a) Initial unlocked $^{31}P\{^1H\}$ NMR spectrum of **^{PO}Cb** and [Ph_3PNPPh_3][PF_6] in DCE. (b) $^{31}P\{^1H\}$ NMR spectrum of the DCE layer following GBE charging generating the reduced **[^{PO}Cb]$^{2-}$** and some residual **^{PO}Cb**. (c) $^{31}P\{^1H\}$ NMR spectrum of DCE layer following the selective UO_2^{2+} capture from the aqueous layer containing $UO_2(NO_3)_2(THF)_2$, $Th(NO_3)_4$•H_2O, $Nd(NO_3)_3THF_3$, $Sm(NO_3)_3THF_3$, and $CsNO_3$ in 0.5 M NaOAc buffer (pH = 5.4), indicating the formation of **[UO_2(^{PO}Cb)$_2$]$^{2-}$**, as well as some minor **^{PO}Cb** and **[Bu_4N][^{PO}CbH]** (denoted as *). No resonances attributable to the captured metal anions, **[Cs(^{PO}Cb)]$^-$** (31.7 ppm), **[Nd(^{PO}Cb)$_3$]$^{3-}$** (140.6 ppm), **[Sm(^{PO}Cb)$_3$]$^{3-}$** (27.9 ppm), or **[Th(^{PO}Cb)$_3$]$^{2-}$** (51.3 ppm), are observed (inset). (d) ^{31}P{^{1}H} NMR spectrum of the DCE layer following GBE discharging revealing a very broad resonance at 23 ppm which we attribute to an adduct of UO_2^{2+} with **^{PO}Cb**.[5] (e) ^{31}P{^{1}H} NMR spectrum of the DCE layer following UO_2^{2+} release by mixing with fresh NaOAc buffered solution (0.1 M) after 15 h and revealing the free carborane **^{PO}Cb** (major), as well as an unknown by-product at 20 ppm, marked by *.

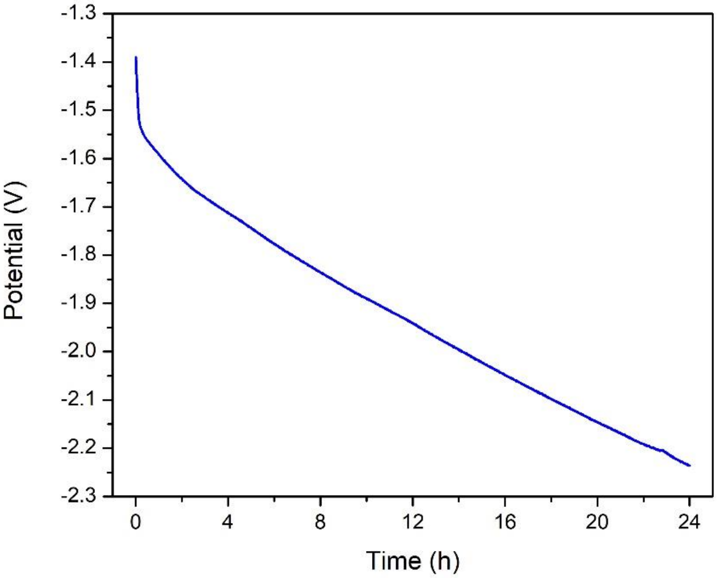

Figure S5. Charging Curve for the Electrochemical Capture of UO_2^{2+}. A charging current of -107.1 μA was applied for a total of -9.25 C of charge transferred, resulting in a 76% SOC after 24 h assuming 100% columbic efficiency.

Selective UO_2^{2+} Capture: A 60 mL plastic bottle was loaded with either 0.39 or 0.19 mmols of each of $Th(NO_3)_4{\bullet}H_2O$, $Nd(NO_3)_3THF_3$, $Sm(NO_3)_3THF_3$, $CsNO_3$ and crystalline $UO_2(NO_3)_2(THF)_2$ dissolved in 25 mL of Milli-Q water (pH = 2.6) or a 0.5 M NaOAc buffered solution (pH = 5.4) resulting in a bright yellow-green stock solution. A 5 mL aliquot of the stock solution (1.25 or 0.6 equiv) was added dropwise without stirring to the DCE solution containing the electrochemically reduced $\mathbf{^{PO}Cb^{2-}}$. After addition, the mixture was allowed to stir for 1.5 h, resulting in a bright yellow organic phase and a pale yellow-green aqueous phase. Stirring was discontinued and the organic and aqueous phases were separated using a small separatory funnel. A 0.5 mL aliquot was taken from the yellow DCE layer and transferred to an NMR tube. An unlocked $^{31}P\{^{1}H\}$ NMR spectrum was collected indicating the formation of $\mathbf{[UO_2(^{PO}Cb)_2]^{2-}}$, as well as some $\mathbf{^{PO}Cb}$ and $\mathbf{[Bu_4N][^{PO}CbH]}$, but no resonances attributable to the captured metal anions, $\mathbf{[Cs(^{PO}Cb)]^{-}}$, $\mathbf{[Nd(^{PO}Cb)_3]^{3-}}$, $\mathbf{[Sm(^{PO}Cb)_3]^{3-}}$, or $\mathbf{[Th(^{PO}Cb)_3]^{2-}}$ (**Figure S2c-4c**). The NMR solution was returned to the 20 mL vial.

Oxidation (Discharging): The DCE layer was returned to the H-cell and GBE was used to discharge (oxidize) the carborane, initiating UO_2^{2+} release. A discharging current of 107.1 μA with a 9.25 C charge cutoff was utilized resulting in a final SOC of ca. 0 % (**Figure S6**; assuming 100% columbic efficiency and no loss of material during the biphasic capture). Upon completion, a 0.5 mL aliquot was taken from the pale yellow DCE layer and transferred to an NMR tube. An unlocked $^{31}P\{^{1}H\}$ NMR spectrum was collected indicating a very broad signal between 35–40 ppm which we attribute to an adduct of UO_2^{2+} with $\mathbf{^{PO}Cb}$ (**Figure S2d-S4d**).[5] The NMR sample and working compartment solutions were combined and placed in a 20 mL vial for subsequent release chemistry.

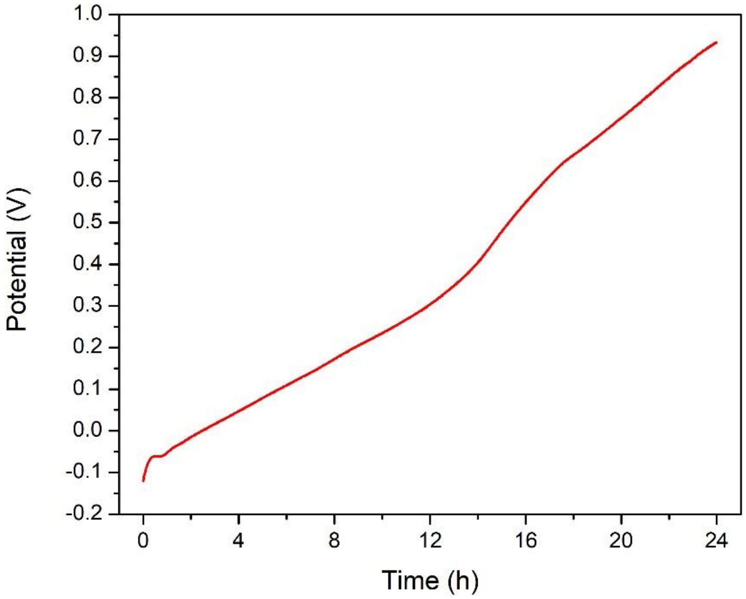

Figure S6. Discharging Curve for the Electrochemical Release of UO_2^{2+}. A discharging current of 107.1 μA was applied for a total of ca. 9.25 C of charge transferred, resulting in a 0% SOC after 24 h assuming 100% columbic efficiency.

UO_2^{2+} recovery: The 20 mL vial containing the electrochemically discharged DCE solution was equipped with a stir bar and a 5 mL solution of 0.1 M NaOAc buffer or Milli-Q water was added dropwise to it. The mixture was allowed to stir for 15 h, resulting in a bright-yellow aqueous phase and a colorless organic layer. A 0.5 mL aliquot was taken from the colorless DCE layer and transferred to an NMR tube. An unlocked $^{31}P\{^1H\}$ NMR spectrum was collected indicating the clean formation of **^{PO}Cb**, $[Ph_3PNPPh_3][PF_6]$, and a small unknown by-product at 20.1 ppm (denoted as *) (**Figure S2e-S4e**).

Control: 5 mL of the stock solution was stirred with 6 mL of a 0.1 M solution of $[Bu_4N][PF_6]$ in DCE for 1.5 hours. The aqueous solution was isolated from the DCE layer and saved for analysis by ICP-OES. The DCE layer was then stirred with either 0.1 M NaOAc buffer or Milli-Q water for 15 h. The aqueous solution was isolated from the DCE layer and saved for analysis by ICP-OES.

S4. Supplementary Figures for X-Ray Crystallography

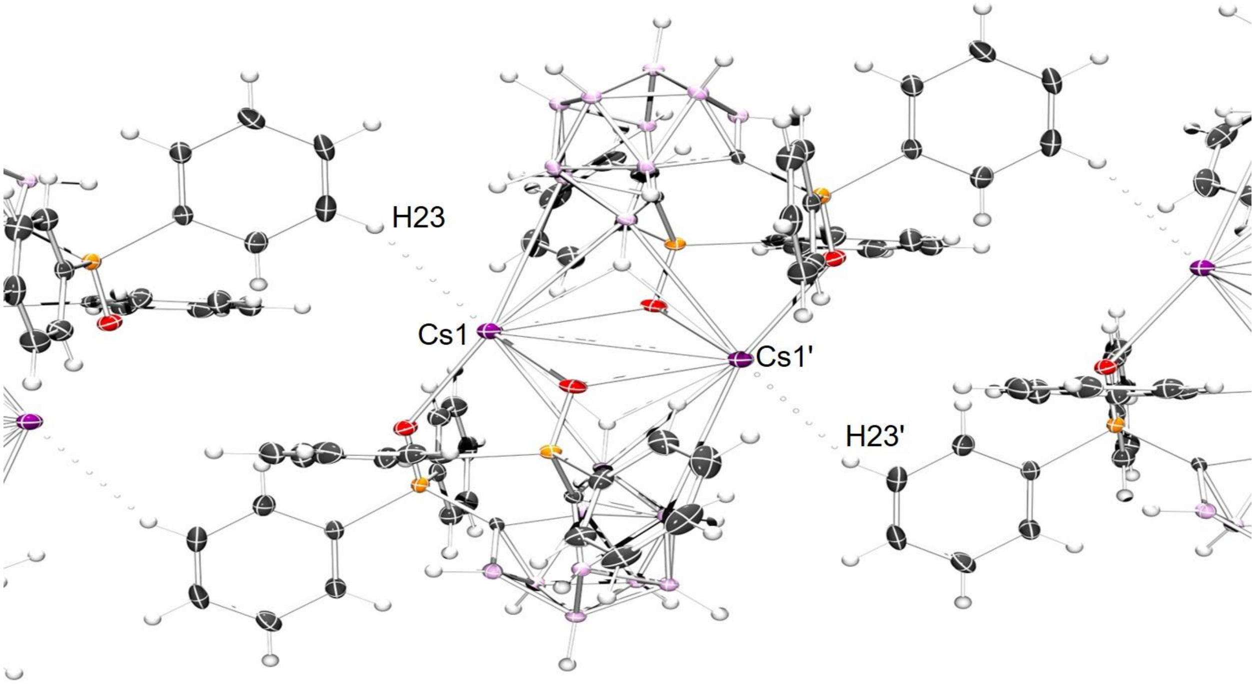

Figure S7. Solid-state molecular structure of **[[CoCp$^*_2$][Cs(^{PO}Cb)]]$_2$** displaying polymeric structure through long Cs1-H23 contacts (3.199 Å). [CoCp$^*_2$]$^+$ counter cations are omitted for clarity.

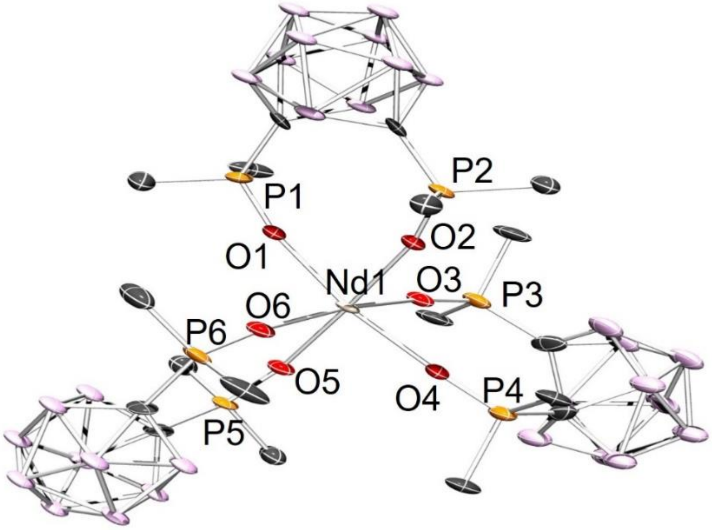

Figure S8. Solid-state molecular structure of **[CoCp$^*_2$]$_3$[Nd(^{PO}Cb)$_3$]**. H atoms, [CoCp$^*_2$]$^+$ counter cations, phenyl C–H linkages, and all co-crystallized solvent molecules are omitted for clarity.

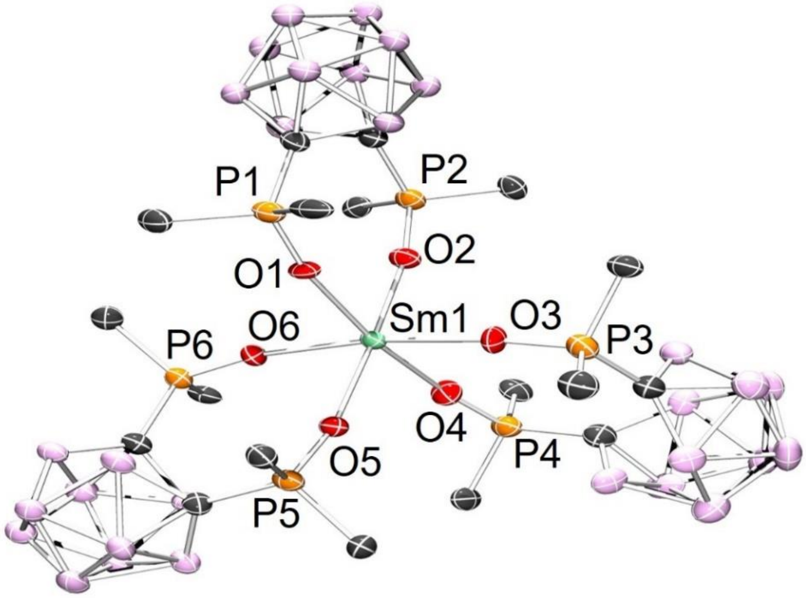

Figure S9. Solid-state molecular structure of **$[\mathrm{CoCp}^*_2]_3[\mathrm{Sm}(^{\mathrm{PO}}\mathrm{Cb})_3]$**. H atoms, $[\mathrm{CoCp}^*_2]^+$ counter cations, phenyl C–H linkages, and all co-crystallized solvent molecules are omitted for clarity.

S5. Supplementary Figures for NMR Spectroscopy

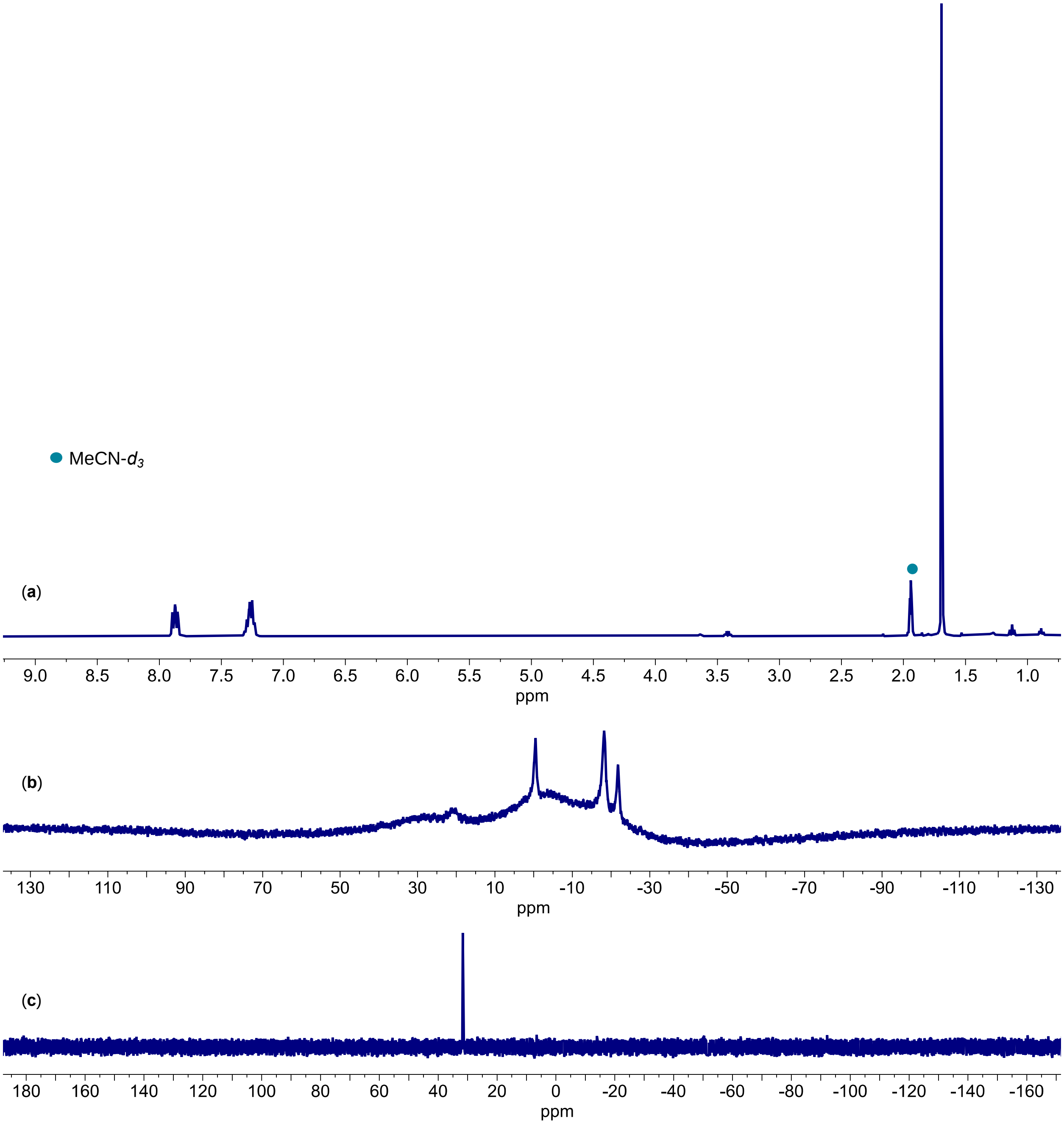

Figure S10. (**a**) ^{1}H NMR (400 MHz) spectrum of **[[CoCp$^{*}_{2}$][Cs(^{PO}Cb)]]$_2$** in MeCN-d_3. (**b**) ^{11}B{^{1}H} NMR (128 MHz) spectrum of **[[CoCp$^{*}_{2}$][Cs(^{PO}Cb)]]$_2$** in MeCN-d_3. (**c**) ^{31}P{^{1}H} NMR (162 MHz) spectrum of **[[CoCp$^{*}_{2}$][Cs(^{PO}Cb)]]$_2$** in MeCN-d_3.

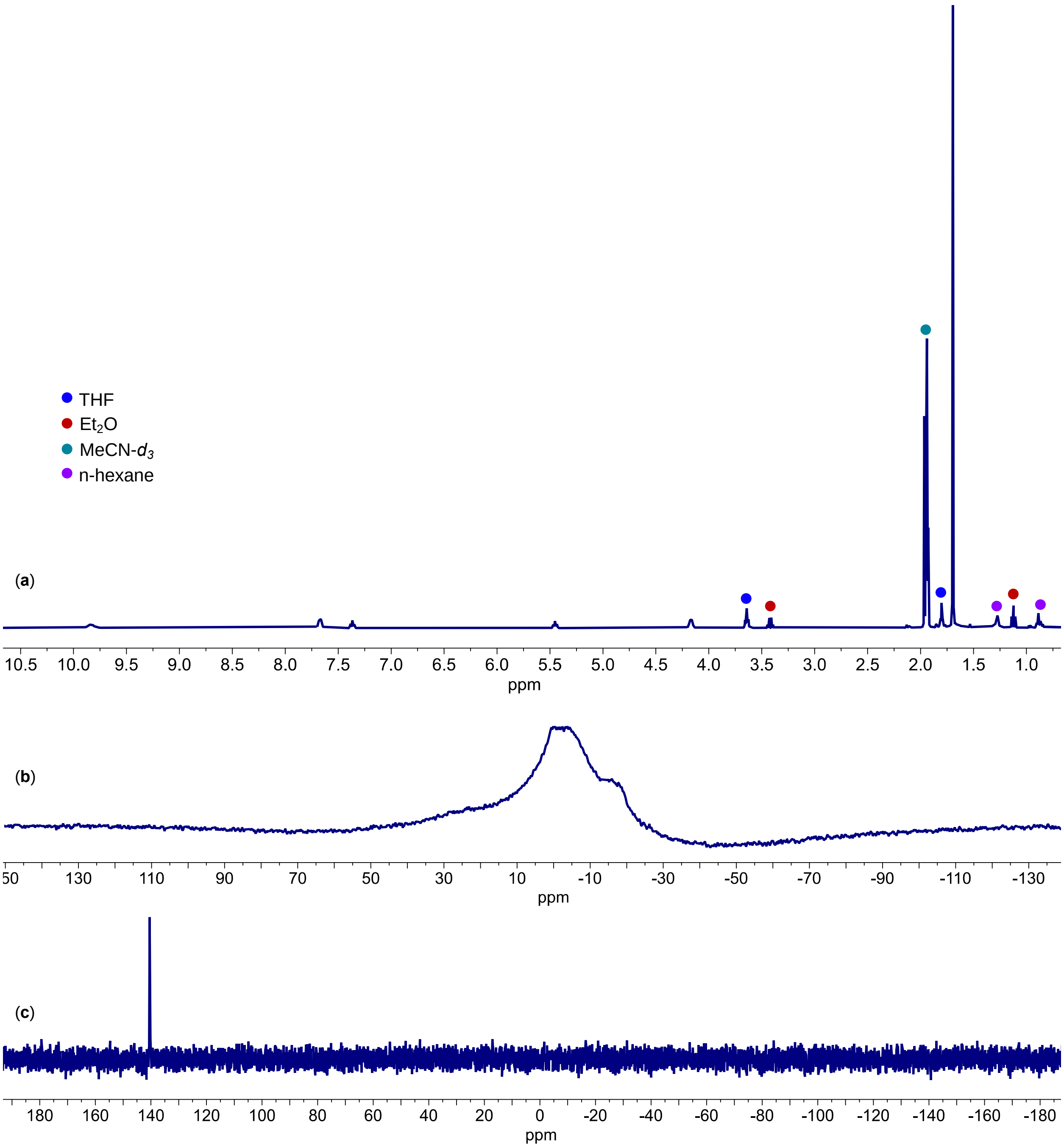

Figure S11. (**a**) ^{1}H NMR (400 MHz) spectrum of **[CoCp$^*_2$]$_3$[Nd(^{PO}Cb)$_3$]** in MeCN-*d*$_3$. (**b**) ^{11}B{^{1}H}NMR (128 MHz) spectrum of **[CoCp$^*_2$]$_3$[Nd(^{PO}Cb)$_3$]** in MeCN-*d*$_3$. (**c**) ^{31}P{^{1}H} NMR (162 MHz) spectrum of **[CoCp$^*_2$]$_3$[Nd(^{PO}Cb)$_3$]** in MeCN-*d*$_3$.

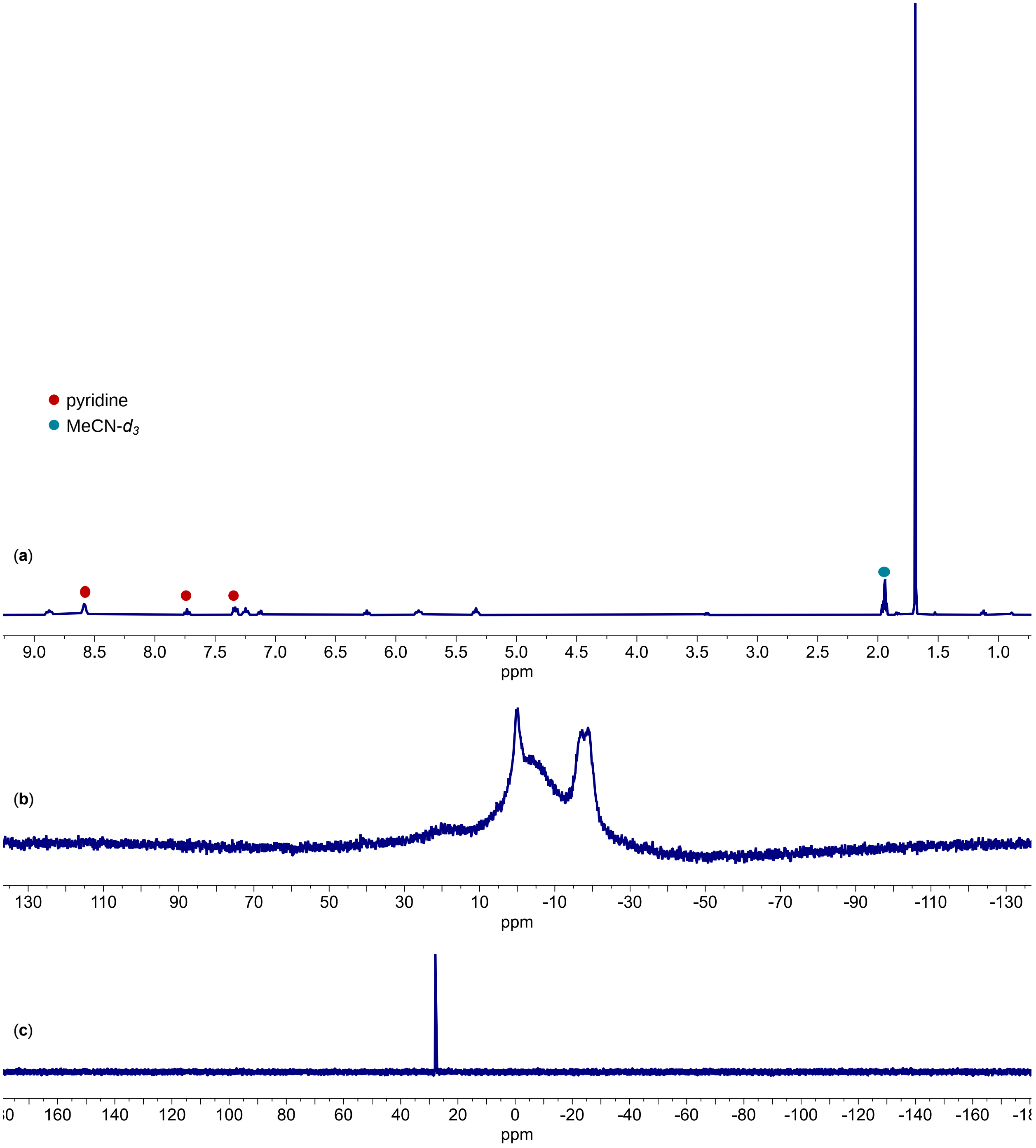

Figure S12. (**a**) ^{1}H NMR (400 MHz) spectrum of **[CoCp$^*_2$]$_3$[Sm(^{PO}Cb)$_3$]** in MeCN-d_3. (**b**) ^{11}B{^{1}H} NMR (128 MHz) spectrum of **[CoCp$^*_2$]$_3$[Sm(^{PO}Cb)$_3$]** in MeCN-d_3. (**c**) ^{31}P{^{1}H} NMR (162 MHz) spectrum of **[CoCp$^*_2$]$_3$[Sm(^{PO}Cb)$_3$]** in MeCN-d_3.

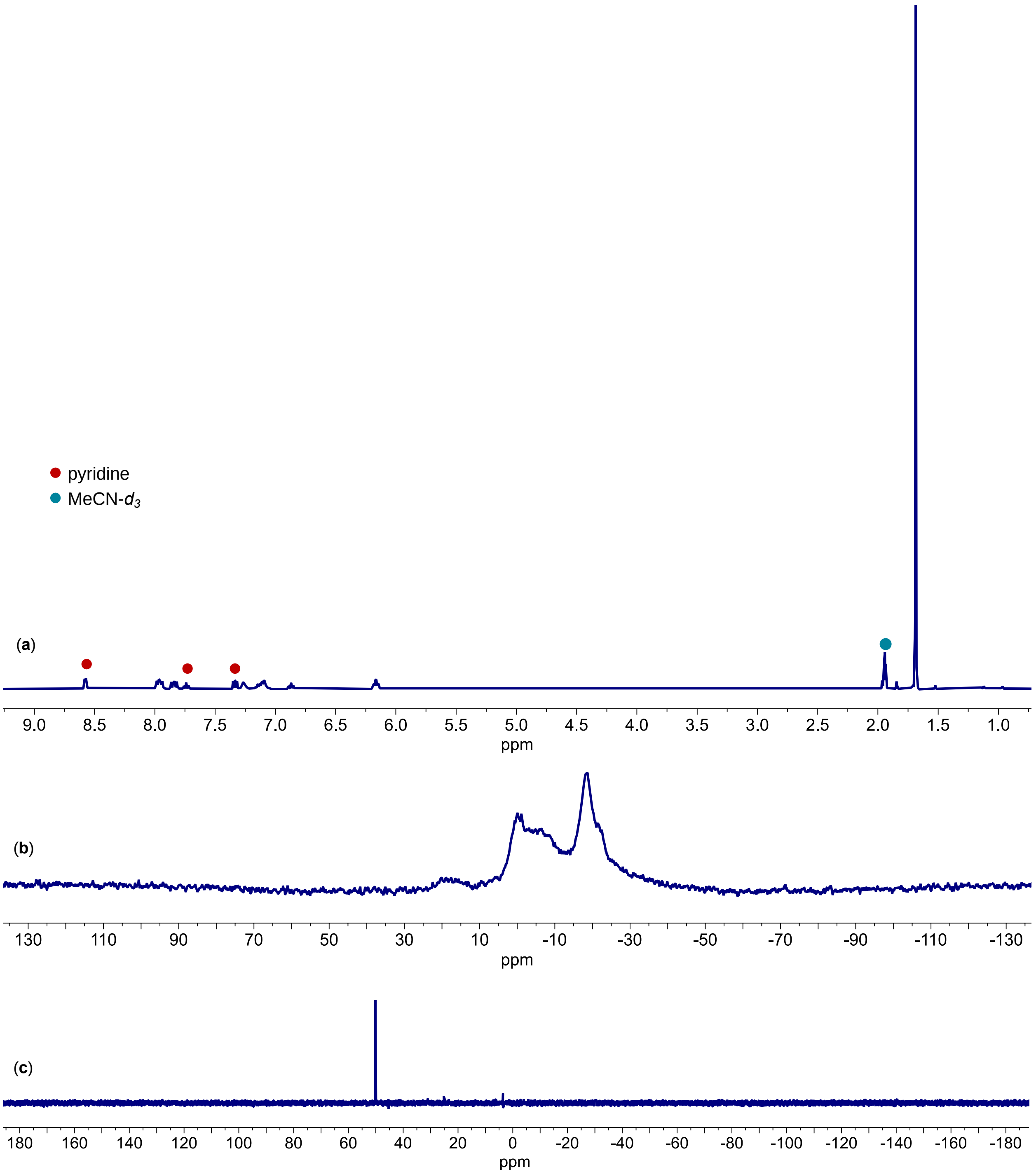

Figure S13. (**a**) ^{1}H NMR (400 MHz) spectrum of **[CoCp$^*_2$]$_2$[Th(^{PO}Cb)$_3$]** in MeCN-d_3. (**b**) ^{11}B{^{1}H} NMR (128 MHz) spectrum of **[CoCp$^*_2$]$_2$[Th(^{PO}Cb)$_3$]** in MeCN-d_3. (**c**) ^{31}P{^{1}H} NMR (162 MHz) spectrum of **[CoCp$^*_2$]$_2$[Th(^{PO}Cb)$_3$]** in MeCN-d_3.

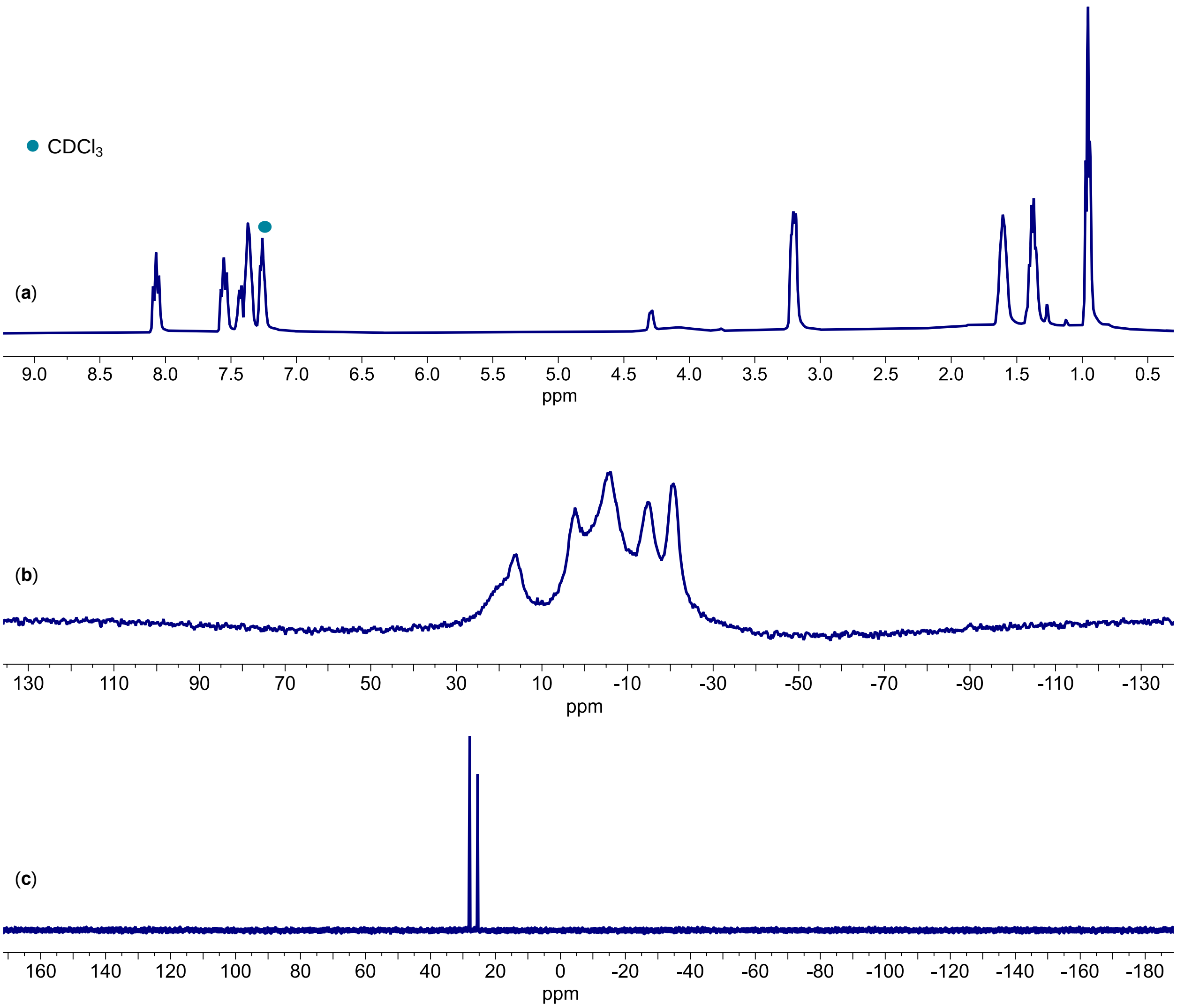

Figure S14. (**a**) ^{1}H NMR (400 MHz) spectrum of **[Bu$_4$N][^{PO}CbH]** in CDCl$_3$. (**b**) ^{11}B{^{1}H} NMR (128 MHz) spectrum of **[Bu$_4$N][^{PO}CbH]** in CDCl$_3$. (**c**) ^{31}P{^{1}H} NMR (162 MHz) spectrum of **[Bu$_4$N][^{PO}CbH]** in CDCl$_3$.

S6. References

1. J. G. Reynolds, A. Zalkin and D. H. Templeton, *Inorg. Chem.*, 1977, **16**, 3357-3359.
2. W. J. Evans, D. G. Giarikos, P. S. Workman and J. W. Ziller, *Inorg. Chem.*, 2004, **43**, 5754-5760.
3. J. M. Lalancette, G. Rollin and P. Dumas, *Can. J. Chem.*, 1972, **50**, 3058-3062.
4. Y. Liu, W.-M. Ren, C. Liu, S. Fu, M. Wang, K.-K. He, R.-R. Li, R. Zhang and X.-B. Lu, *Macromolecules*, 2014, **47**, 7775-7788.
5. M. Keener, C. Hunt, T. G. Carroll, V. Kampel, R. Dobrovetsky, T. W. Hayton and G. Ménard, *Nature*, 2020, **577**, 652-655.
6. G. Sheldrick, *Acta Cryatallogr. A*, 2015, **71**, 3-8.
7. G. Sheldrick, *Acta Cryatallogr. C*, 2015, **71**, 3-8.
8. O. V. Dolomanov, L. J. Bourhis, R. J. Gildea, J. A. K. Howard and H. Puschmann, *J. Appl. Crystallogr.*, 2009, **42**, 339-341.
9. J. Chlistunoff, K. J. Ziegler, L. Lasdon and K. P. Johnston, *J. Phys. Chem. A*, 1999, **103**, 1678-1688.